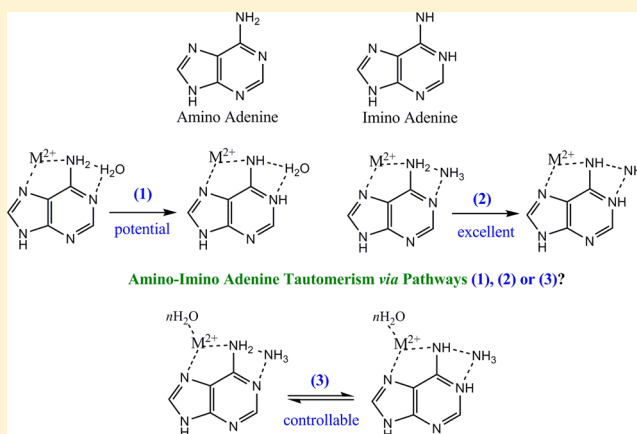


Amino–Imino Adenine Tautomerism Induced by the Cooperative Effect between Metal Ion and H<sub>2</sub>O/NH<sub>3</sub>Hongqi Ai,<sup>\*,†</sup> Jinpeng Chen,<sup>†</sup> and Chong Zhang<sup>‡</sup><sup>†</sup>Shandong Provincial Key Laboratory of Fluorine Chemistry and Chemical Materials, School of Chemistry and Chemical Engineering, University of Jinan, Jinan City, 250022, P. R. China<sup>‡</sup>Department of Chemistry and Technology, Liaocheng University, Liaocheng 252059, P. R. China

## S Supporting Information

**ABSTRACT:** Tautomerization processes of amino–imino adenine isomer (A → A1) in five different environments are studied by the density functional theory (B3LYP) method. The five environments are metal ion (M, M = K<sup>+</sup>, Na<sup>+</sup>, Cu<sup>+</sup>, Zn<sup>+</sup>, Ca<sup>2+</sup>, Mg<sup>2+</sup>, Cu<sup>2+</sup>, Zn<sup>2+</sup>) coordinated bidentate system, either monowater (W) or monoammonia (N) attached system, both metal ion and monowater cooperative system (M-W), and both metal ion and monoammonia cooperative system (M-N). Results show that the complexes formed by noncanonical rare imino form A1 are more stable than those formed by the canonical amino one in most of these environments. The tautomerization of A → A1 becomes quite easy in either M-W or M-N system. It is noteworthy that under divalent M-N environment the A → A1 process meets with particularly lower and even free energy barrier, indicating the instability of the amino adenine isomer and probable existence of more stable imino adenine isomer. Expanding studies for the microhydration at the metal ion of the M-N system predict the required number (*n*) of water molecules to remain the amino adenine isomer A (AMN<sub>*n*</sub>W) stable. The number of *n* is 2, 3, 3, and 4 for M = Ca<sup>2+</sup>, Zn<sup>2+</sup>, Cu<sup>2+</sup>, and Mg<sup>2+</sup>, respectively. The present study provides further understanding for the amino–imino tautomerization behavior of the most stable adenine under the influence of several related closely factors, and is useful for rational design of these different environments for the purposes of prevention and control of pyrimidines mispairing, which is responsible for the mutagenic properties of the nucleic acid bases.



## 1. INTRODUCTION

Tautomerization of a nucleic acid base between its canonical form and noncanonical tautomeric one plays a crucial role in the point mutation.<sup>1–14</sup> Generally, the noncanonical form has much higher energy than the canonical one,<sup>15–20</sup> and usually the tautomerization process has to overcome a very huge activation energy barrier. However, some influence factors, such as hydration,<sup>15–18,20–26</sup> protonation,<sup>19</sup> and metal binding,<sup>27–30</sup> will make such tautomerization take place readily; and as a result, existence of the noncanonical form with higher energy becomes probable even though it is scarce.<sup>31,32</sup> Both experimental and theoretical results have verified that the noncanonical forms can lead to mispairing of pyrimidines and purines, which is responsible for the mutagenic properties of the nucleic acid bases.<sup>33–41</sup>

As one of four common bases, adenine in Watson–Crick base pairs exists in canonical form (A) generally.<sup>1,3,6,11,14,15,19,20,28,35,40</sup> The canonical form is characterized by an amino group. It can produce several different tautomeric forms by transferring a proton from its amino group to a neighboring nitrogen site and thus becomes a noncanonical

form, the rare imino form (A1/2),<sup>6,15,42,43</sup> for instance. The structural distinction between the amino and imino forms lies in different locations of H15; i.e., H15 locates at N10 site in the most stable amino adenine A and it would shift to the N1 site in the high-energy imino form A2. If the remainder H14 of A2 further rotates around the C6–N10 bond to the opposite side, then A1 can be obtained (Figure 1). Obviously, the A → A2 → A1 process can hardly occur due to unfavorable thermodynamics (relative energy rank,  $E_A < E_{A2} < E_{A1}$ <sup>15,20,31</sup>) and kinetics conditions.<sup>20,35,39,44,45</sup> It has been confirmed that the imino form A2 is one of many potential isomers to induce lethal mutation of adenine in nucleobase mispairings, such as in AT → A2T,<sup>35,39,44,45</sup> AT → CG, or AT → A2C transitions.<sup>31,45,46</sup> Most importantly, such lethal mutation is unrepairable.<sup>47</sup> This indicates that there must be some factors to induce these tautomerization processes, which are in sore need of investigation.

Received: June 21, 2012

Revised: October 29, 2012

Published: October 30, 2012

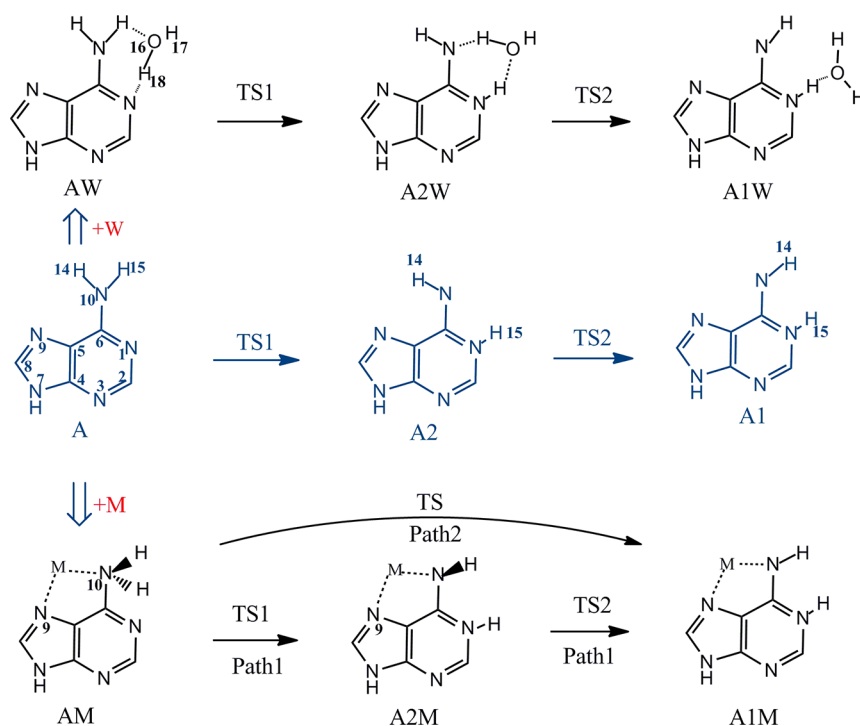


**Figure 1.** Atomic labels of adenine and schematic representation of the molecules as well as the different reaction mechanisms in the tautomerization processes of A → A1 in M and W systems.

Metalation can lead to intramolecular proton transfer (PT) of canonical adenine A and, as a result, the base mutates into a rare one. In detail, a metal entity can replace the proton H15 at the exocyclic amino group (N10) of adenine A and generate a bidentate metal complex, in which H15 has to shift to N1 site and results in the higher-energy imino tautomer (A1/A2).<sup>46,48</sup> The two imino adenine isomers can be stabilized firmly by coordinating a metal ion (M) at its both N9 and N10 sites. Interestingly, the product A1M is more stable than the complex AM.<sup>32,42,43,46,48–52</sup> A 1:1 complex formed between Cu<sup>2+</sup> and N10 of adenine A in an analogue of adenosine 5'-monophosphate was determined<sup>53</sup> experimentally in early 1993. In some studies<sup>47,54,55</sup> on antitumor compounds, it was also found that the dirhodium–A1 complex with both a Rh–Rh bonding and the two metal ions binding respectively at the N9 and N10 sites of A1 was the most stable.

Previous studies<sup>20,22,23,25</sup> also observed that water could make the tautomerization equilibrium move toward the rare ones. For example, a 1:1 structure of water–adenine, in which the water molecule is bridged between H14 and N9 of the adenine, had been predicted experimentally in 1971.<sup>56</sup> Interaction with a water molecule (W)<sup>20</sup> can indeed enhance the stability of the imino adenines, yet the interaction cannot render the imino forms (A1W/A2W) more stable than the amino one (AW). On the other hand, the interaction can also greatly lower the energy barrier of PT process, indicating that the water molecule attachment promotes the kinetic process rather than the thermodynamic one. Hanus et al.<sup>15</sup> once theoretically predicted that hydration could enhance the relative stability of the imino adenine forms in either a microhydrated environment (one or two water molecules) or a bulk water environment, further supporting the rare tautomer hypothesis of substitution mutagenesis in aqueous phase.<sup>33</sup>

Cooperative effects of both hydration and metal ion binding are often concerned important factors to the amino–imino

tautomerization process.<sup>57,58</sup> Hu et al.<sup>57</sup> once probed the cooperative effect of both water molecules and Na<sup>+</sup> on the stability of uracil isomers and found that the cooperative effect could maintain the classical uracil base stable; i.e., it was more difficult for the uracil to tautomerize in the metal ion–water cooperative environment (M–W) than in only water molecule(s) assisted one. Michalkova et al.<sup>58</sup> reported thermodynamics and kinetics of amino–imino tautomeric transition in N1–methyl–cytosine in the presence of both Na<sup>+</sup> and up to two water molecules. Our group<sup>59</sup> in 2009 investigated the catalysis effects of both water molecules and charges on intramolecular PT of uracil. As a partner in mispaired AT → A2C, AT → A2G<sub>syn</sub><sup>31,35,46,47</sup> and AT → A2T,<sup>47</sup> adenine tautomerization in such a W–M environment would also be an interesting issue.

In addition to those mentioned above, ammonia (N) can also affect the tautomerization process of adenine.<sup>19</sup> Protonated amino groups are ubiquitous in biological systems, such as protonated amino acids, peptides, and proteins, as well as DNA and RNA.<sup>19</sup> For example, in structures and sequences of individual DNA base–amino acid interactions, asparagine had been determined to bind adenine preferentially by Jernigan groups<sup>60</sup> due to its side chain without net charge,<sup>61</sup> indicating its amido group is the most potential candidate to interact with the adenine. The interactions between DNA and proteins are critical to gene expression and regulation, and of significant importance for possible therapeutic strategies. Thus, an ammonia molecule would be a suitable simplification model to bind an adenine so that a deep insight into such interaction can be obtained. Currently, most of research groups only focus on the tautomerization process under the condition of one of the above factors; a study of the process with two and even more cooperative factors<sup>19,57–59</sup> would offer more valuable information, however.

In the present paper, we aim to investigate the tautomerization processes between A, the most stable isomer of adenine,<sup>1,3,6,11,14,15,19,20,28,35,40</sup> and A1, the reactant of the most stable adenine–metal complex,<sup>32,42,43,46,48–52</sup> influenced by following cooperative factors, M–W, M–N, and M–N<sub>n</sub>W ( $n = 1–4$ ), respectively. The metal ions involved are four univalent, K<sup>+</sup>, Na<sup>+</sup>, Cu<sup>+</sup>, and Zn<sup>+</sup>, and four divalent, Ca<sup>2+</sup>, Mg<sup>2+</sup>, Cu<sup>2+</sup>, and Zn<sup>2+</sup>, the most familiar ones in vivo.<sup>28,29,32,42,43,48–52,62</sup> In order to compare the cooperative effect conveniently, single factor (either W/N or M) involved system will be also considered. Due to the favorable stability of A1M over AM,<sup>32,42,43,48,50–52</sup> the thermodynamics process in the metal-ion-induced tautomerization of A → A2 → A1 has received extensive attention;<sup>32,42,43,48,50–52</sup> the corresponding kinetic process still remains unknown, however, not least the tautomerization process under the cooperative M–W and M–N circumstances. Would the tautomerization become more available or not in both thermodynamics and kinetics for the AM → A1M in the case of W, N, or both of them with further attachment? We hope to find the answer by this study.

## 2. COMPUTATIONAL METHODS

AW and AN complexes are generated by using a water and an ammonia molecule to bind H15 of A, respectively, to promote PT from the N10 site to the N1 one. Once PT is completed, the products of A2W/A2N and A1W/A1N complexes can be obtained.<sup>15,19,20</sup> As a scheme, AW in Figure 1 shows the atomic labels and the binding sites of a water molecule to the adenine. Likewise, an ammonia molecule is also put here (not shown in this figure) to bridge N1 and H15 of A so that the proton transfers more smoothly. A series of metalated complexes AM and A1M can be obtained by these different metal cations to bind bidentately at the N9 and N10 sites of A and A1/2, as the bidentate coordination is the most favorable to the stability of A and A1.<sup>32,42,43,48–52</sup> On the basis of structures of AM/A1M, AMW(N)/A1MW(N) can be generated by further attaching a water or an ammonia molecule at their H15 site, as we have done to produce AW/AN. Depending on different properties of metal ion bound, the process of AMW(N) → A1MW(N) may be achieved by path 1 or 2. For path 1, an intermediate product has to be included, as shown in the AM → A2M → A1M process in Figure 1. Detailed discussions are displayed everywhere in the following text.

All structures in these tautomerization processes, A → A2 → A1, AM (→A2M) → A1M(M system), AW → A2W → A1W(W system), AN → A2N → A1N (N system), AMW (→A2MW) → A1MW (M–W system), and AMN → A1MN(M–N system), are optimized with the Becke3 (B3) exchange<sup>63</sup> and Lee–Yang and Parr (LYP) correlation<sup>64</sup> potentials in combination with 6-31G(d) basis set, as the DFT method can describe well the geometrical parameters and energetic values in the similar base systems.<sup>20,21,57</sup> Frequency calculations are also carried out at the same level to identify the stationary structures and transition states (TSs), in which zero-point vibrational energy (ZPVE) can be determined. Meanwhile, calculation of intrinsic reaction coordinate<sup>65</sup> (IRC) is also performed for each TS at the same level. Single-point calculations are further considered at the B3LYP/6-311++G(d,p) level to refine the energetic values. The basis set superposition errors (BSSEs)<sup>66</sup> are contained in all these binding energy calculations. Subsequently, the transfer processes of both H15 and the ammonia molecule along with the stretch of N10–N16 (NH<sub>3</sub>) distance in AMN (M = Mg<sup>2+</sup>,

Cu<sup>2+</sup>, Zn<sup>2+</sup>) complexes have been investigated by scanning their potential energy surface (PES) at the B3LYP/6-31G(d) level. The corresponding structural changes along with N10–N16 distance stretch are listed in Figures S1–S3 of the Supporting Information. A reoptimization at the M062x level<sup>67</sup> in combination with larger basis set 6-311++G(d,p) (than 6-31G(d) employed above) is further performed to verify such a process (Figure S2-3). M062x/6-311++G(d,p) is also employed to calculate the microhydrated AMN → A1MN processes since the M062x had been confirmed to perform better than B3LYP in systems where main-group thermochemistry, kinetics, and noncovalent interactions are all important.<sup>67</sup> Moreover, a recent study on the exocyclic DNA adducts reported that B3LYP underestimated the hydrogen-bonding strength as compared with the M062x method which was in good agreement with other references.<sup>68</sup> For the 7-azaindole-(H<sub>2</sub>O)<sub>n'</sub> ( $n' = 1,2$ ) complexes, which are very close in structure and in interaction mode to present microhydrated complexes in AMN<sub>n</sub>W → A1MN<sub>n</sub>W ( $n = 1–4$ ) processes, Fang and Kim's report<sup>69</sup> revealed that M062x/6-311++G(d,p) predicted the TSs successfully in the processes of their excited-state tautomerization, whereas B3LYP/6-311++G(d,p) failed.

The electronic stabilization energy ( $\Delta E_{\text{Stab}}$ )<sup>32</sup> in different systems is defined as

$$\text{in M bound systems, } \Delta E_{\text{Stab}} = \Delta E_{\text{BE}}^{\text{M}} + \Delta E_{\text{Def}} \quad (1)$$

in W or N(W/N) attached systems,

$$\Delta E_{\text{Stab}} = \Delta E_{\text{BE}}^{\text{W/N}} + \Delta E_{\text{Def}} \quad (2)$$

in M–W cooperative systems,

$$\Delta E_{\text{Stab}} = \Delta E_{\text{BE}}^{\text{M}} + \Delta E_{\text{BE}}^{\text{W}} + \Delta E_{\text{Def}} \quad (3)$$

in M–N cooperative systems,

$$\Delta E_{\text{Stab}} = \Delta E_{\text{BE}}^{\text{M}} + \Delta E_{\text{BE}}^{\text{N}} + \Delta E_{\text{Def}} \quad (4)$$

where  $\Delta E_{\text{BE}}^{\text{M}}$ ,  $\Delta E_{\text{BE}}^{\text{W}}$ , and  $\Delta E_{\text{BE}}^{\text{N}}$  denote the electronic vertical binding energies of M, W, and N to A/A1/A2 or AM/A1M/A2M complexes, respectively;  $\Delta E_{\text{Def}}$  is the deformation energy of A/A1/A2 induced by the binding of M (eq 1) or by attachment of either W/N (eq 2) or both M and W/N (eqs 3 and 4). Consequently, the component choice in the BSSE computations depends on the binding energy computation for which part in the three-body M–W/N cooperative systems. In detail, if the binding energy is for W in the M–W system, then the two components are W and AM/A1M/A2M complex, respectively; if it is for M, then the two components become M and the corresponding AW/A1W/A2W complex, respectively.

All calculations are performed with the Gaussian 09 package of programs.<sup>70</sup>

## 3. RESULTS AND DISCUSSION

As an isomer of A, A2 is also considered as it plays an intermediate role during the transformation process of A → A1 and is a common isomer in DNA mismatched pairs.<sup>31,35,46,47</sup> The corresponding structures are shown in Figure 1.

### 3.1. Metal-Ion-Induced Intramolecular PT Process.

The tautomerization process of A → A1 undergoes two steps, A → A2 and A2 → A1 (Figure 1 and Figure S4 in the Supporting Information). The energies of product A1 and intermediate A2 are 18.6 and 12.4 kcal/mol respectively more than that of the most stable isomer of adenine A,<sup>3,6</sup> which are in



good agreement with the available theoretical results.<sup>3,15,20,42,50,54</sup> In the first step, H15 at N10 site of A is transferred to N1 site and the C6–N10–H14 angle turns from 120.4° to 109.1°, forming the intermediate A2. In the second step, H14 is rotated from the initial position to produce planar tautomer A1. The ZPVE-corrected activation energies in the two steps are 45.4 and 23.4 kcal/mol, respectively. The large energy barrier of the PT process indicates that tautomerization hardly occurs in such circumstances.<sup>20</sup> On the other hand, H14 transfer from the N10 site to the N9 site seems more obtainable due to lower energy barrier (8.0 kcal/mol).<sup>3</sup>

The activation energies of these PT processes change in M-bound systems, however, and the changes (Figure S4 in the Supporting Information) depend on the sort and charge of metal ion bound. For the systems involving monovalent alkali metal, two-step tautomerization processes in both  $\text{ANa}^+ \rightarrow \text{A2Na}^+ \rightarrow \text{A1Na}^+$  and  $\text{AK}^+ \rightarrow \text{A2K}^+ \rightarrow \text{A1K}^+$  still persist and the first step is still the rate-determining one due to its higher activation energy (46.2 versus 44.7 kcal/mol) (3.9 versus 7.5 in the second step). Obviously, binding of metal ion leads to minor fluctuation of activation energy in the first step and large decrease in the second one, compared with the counterparts in the  $\text{A} \rightarrow \text{A2} \rightarrow \text{A1}$  process. The results signify that bidentate coordination of metal ion at the N9 and N10 sites hardly improves the first-step  $\text{AM} \rightarrow \text{A2M}$  tautomerization but facilitates the second-step  $\text{A2M} \rightarrow \text{A1M}$  one in kinetics. It is interesting that the  $\text{AM} \rightarrow \text{A1M}$  process does not experience intermediate A2M when  $\text{M} = \text{Cu}^+, \text{Zn}^+, \text{Ca}^{2+}, \text{Mg}^{2+}, \text{Cu}^{2+}$  and  $\text{Zn}^{2+}$ ; i.e., these metal ions can degenerate A into A1 via TS directly (see d,e,...,i in Figure S4) due to their stronger binding energies (Table 1), confirmed by selected optimization processes in Figure S5 in the Supporting Information. A comparison shows that the activation energy decreases in the system involving  $\text{Ca}^{2+}$  (42.0)/ $\text{Mg}^{2+}$  (45.2), whereas it increases in the system involving  $\text{Cu}^{+2+}$  (52.8/50.2)/ $\text{Zn}^{+2+}$  (47.5/45.7), relative to that in the  $\text{A} \rightarrow \text{A2}$  process (45.4 kcal/mol).<sup>20</sup> Generally, coordination of metal ion does not lead to severe change in their tautomerization kinetics.

Energy data of all PT processes are listed in Table 1. Compared with  $\text{A1} < \text{A2} < \text{A}$ , the stability order of the metalated complexes turns into  $\text{A2M} < \text{AM} < \text{A1M}$  for  $\text{Na}^+/\text{K}^+$ -involved complexes. The order becomes  $\text{AM} < \text{A1M}$ , however, for complexes involving other ions ( $\text{Cu}^+, \text{Zn}^+, \text{Ca}^{2+}, \text{Mg}^{2+}, \text{Cu}^{2+}$ , and  $\text{Zn}^{2+}$ ) and agrees well with that of the Nino Russo et al. obtained at the B3LYP/6-311+G(2df,2p) level.<sup>42,50</sup> It indicates that the A1M structures indeed become the most stable ones. To explain the alternation of stability order, stabilization energy ( $\Delta E_{\text{stab}}$ ) is calculated according to eq 1. Data show that the coordination of metal ion generates more stabilization energy for A1 (A1M) than for A (AM), which accounts well for the ordering of their relative energy. The greater stabilization energy of the A1M not only derives from the stronger binding strength of A1–M bond but also from the less deformation of A1 induced by the M bidentate coordination.<sup>32</sup> For example,  $\text{A1Na}^+$  is 7.6 and 21.1 kcal/mol more stable than  $\text{ANa}^+$  and  $\text{A2Na}^+$ , respectively, in good consistency with each corresponding order of stabilization energy [−59.6( $\text{A1Na}^+$ ), −33.3( $\text{ANa}^+$ ), and −32.0 kcal/mol ( $\text{A2Na}^+$ )]. In addition, both stronger corresponding binding energy (−60.8) and lower deformation energy (1.2) of  $\text{A1Na}^+$  than that of  $\text{ANa}^+$  and  $\text{A2Na}^+$  also indicate the A1 structure is more favorable to coordinate a metal ion.

**Table 1. Relative Energy ( $\Delta E$ ), Binding Energy ( $\Delta E_{\text{BE}}^{\text{M}}$ ), Deformation Energy ( $\Delta E_{\text{Def}}$ ) of A/A1, and Stabilization Energy ( $\Delta E_{\text{stab}}$ ) of A/A1/A2M Complexes (Energies in kcal/mol)**

	$\Delta E$	$\Delta E_{\text{BE}}^{\text{M}}$	$\Delta E_{\text{Def}}$	$\Delta E_{\text{stab}}$
A	0.0	—	—	—
A2	11.9, 12.4 <sup>e</sup> , 11.2 <sup>f</sup> , 12.3 <sup>g</sup> , 12.2 <sup>h</sup> , 10.6 <sup>k</sup>	—	—	—
A1	18.6, 19.1 <sup>g</sup> , 18.7 <sup>e</sup> , 18.2 <sup>f</sup> , 18.5 <sup>c,d</sup> , 16.5 <sup>k</sup>	—	—	—
$\text{ANa}^+$	7.6, 7.9 <sup>d</sup>	−44.8	11.5	−33.3, −32.4 <sup>a</sup> , −29.7 <sup>d</sup> , −33.4 <sup>i</sup>
$\text{A2Na}^+$	21.1	−37.7	5.7	−32.0
$\text{A1Na}^+$	0.0	−60.8	1.2	−59.6, −56.1 <sup>a</sup> , −56.3 <sup>d</sup>
$\text{AK}^+$	4.9, 5.1 <sup>d</sup>	−28.5	6.9	−21.6, −18.2 <sup>d</sup> , −22.7 <sup>i</sup>
$\text{A2K}^+$	16.1	−25.9	3.5	−22.4
$\text{A1K}^+$	0.0	−45.8	0.6	−45.2, −42.0 <sup>d</sup>
$\text{ACu}^+$	9.1	−80.4	17.3	−63.1, −66.7 <sup>b</sup> , −64.6 <sup>j</sup>
$\text{A1Cu}^+$	0.0	−95.7	4.7	−91.1
$\text{AZn}^+$	10.3	−71.8	17.9	−53.9, −57.9 <sup>j</sup>
$\text{A1Zn}^+$	0.0	−89.0	6.0	−83.0
$\text{ACa}^{2+}$	24.0, 24.4 <sup>c</sup>	−127.7	17.4	−110.3, 111.5 <sup>c</sup>
$\text{A1Ca}^{2+}$	0.0	−157.0	3.9	−153.1, 154.4 <sup>c</sup>
$\text{AMg}^{2+}$	26.3, 26.6 <sup>c</sup>	−182.9	19.4	−163.5, 156.0 <sup>a</sup> , 165.9 <sup>c</sup>
$\text{A1Mg}^{2+}$	0.0	−216.5	7.9	−208.6, 197.8 <sup>a</sup> , 211.0 <sup>c</sup>
$\text{ACu}^{2+}$	22.1	−268.0	22.1	−245.9, 249.7 <sup>b</sup>
$\text{A1Cu}^{2+}$	0.0	−301.1	14.5	−286.6
$\text{AZn}^{2+}$	27.0	−233.2	21.3	−211.8, 195.6 <sup>a</sup>
$\text{A1Zn}^{2+}$	0.0	−268.4	10.8	−257.6, 238.5 <sup>a</sup>

<sup>a</sup>From ref 32 (RI-MP2/TZVPP). <sup>b</sup>From ref 51 (B3LYP/6-311+G(d,p))/B3LYP/6-31+G(d,p). <sup>c</sup>From ref 50 (at the B3LYP/6-311+G(2df,2p) level). <sup>d</sup>From ref 42 (at the B3LYP/6-311+G(2df,2p) level). <sup>e</sup>From ref 54 (B3LYP/6-311(d,p)). <sup>f</sup>From ref 15 (RI-MP2/TZVPP). <sup>g</sup>From ref 3 (MP2//HF/6-31G(d, p)). <sup>h</sup>From ref 20 (B3LYP/6-311G(d,p)). <sup>i</sup>From ref 49. Experimental results. <sup>j</sup>From refs 43 and 48. <sup>k</sup>From ref 31 (BP86/QZ4P).

**3.2. Intramolecular PT Process in the Monohydrated Systems.** When a water molecule is attached to the adenine isomer in the form of intermolecular hydrogen bonding, it can enhance the relative stability of the noncanonical isomer slightly and lower markedly the activation energy of intramolecular PT reaction. Two activation energies in  $\text{AW} \rightarrow \text{A1W}$  process are shown in Figure 2. As the  $\text{A} \rightarrow \text{A1}$  process (see Figure S4) does,  $\text{AW} \rightarrow \text{A1W}$  also undergoes two steps. By comparing the first step of  $\text{AW} \rightarrow \text{A2W}$  with that of  $\text{A} \rightarrow \text{A2}$  process, it is easily observed that monohydration can decrease the energy barrier of the step by 28.6 kcal/mol and stabilize the noncanonical form by 3.2 kcal/mol, which are in excellent agreement with the B3LYP/6-311G(d,p) results (28.1 versus 3.2 kcal/mol) of Gu and Leszczynski.<sup>20</sup> In the second step  $\text{A2W} \rightarrow \text{A1W}$ , the activation energy is 26.7 kcal/mol and higher by 3.3 kcal/mol than that of  $\text{A2} \rightarrow \text{A1}$ . The relative energies of TSs, AWTS2 and ATS2, to each of their initial reactants AW and A are almost identical (35.9 versus 35.8 kcal/mol), indicating that monohydration can decrease significantly the activation energy of the first step, but has little effect on that of the second step. On the other hand, the difference in activation energy manifests that the second step is the rate-determining one when a water molecule is attached. The

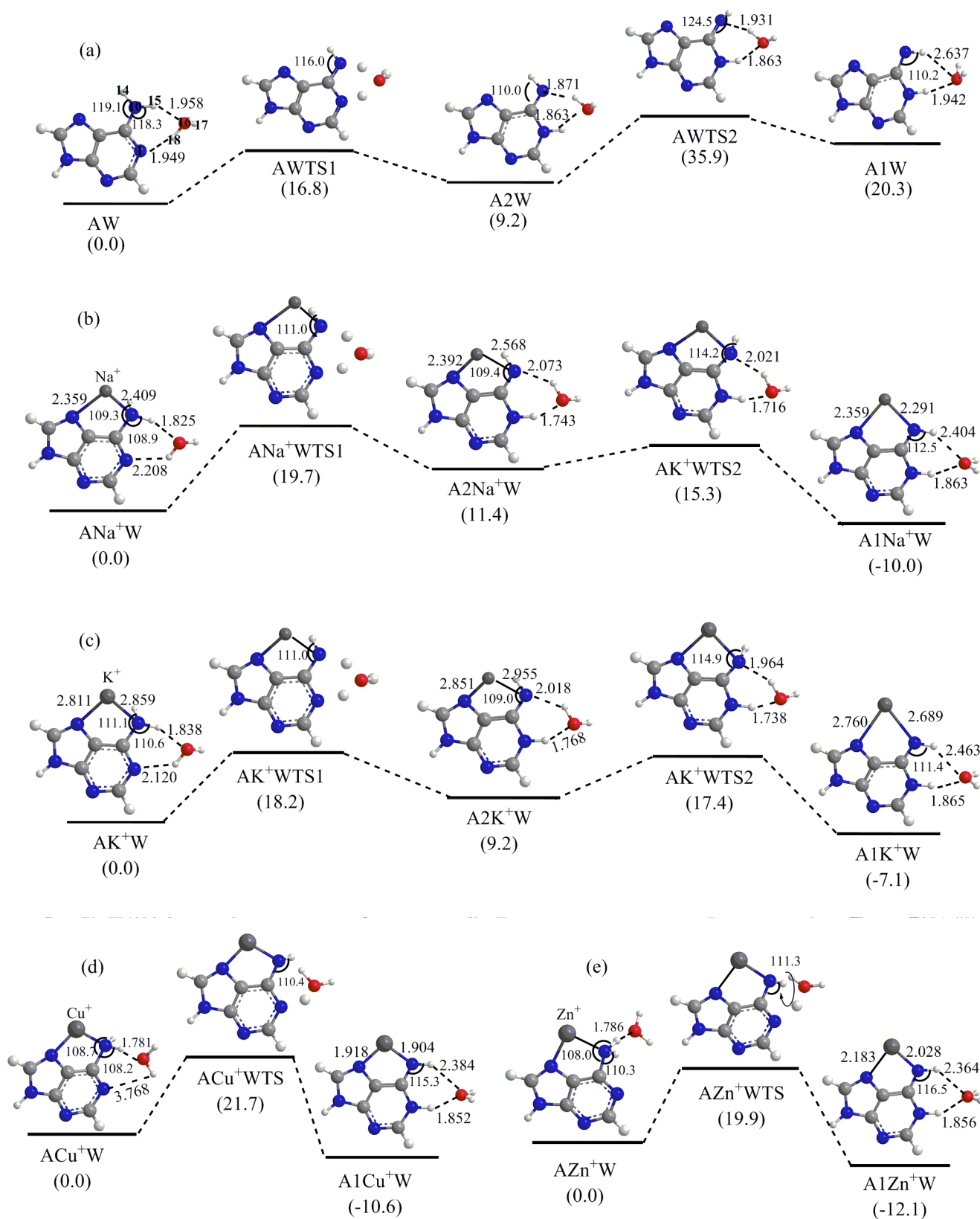


**Figure 2.** Structures and ZPVE-corrected relative energies (in parentheses) in tautomerization processes of AMW ( $\rightarrow$ A2MW)  $\rightarrow$  A1MW. Energy in kcal/mol, distance in angstroms, and angle in degrees.

activation energy in the rate-determining step is 9.5 kcal/mol less than that of non-hydrated  $A \rightarrow A2 \rightarrow A1$  process. Therefore, monohydration improves the  $A \rightarrow A2 \rightarrow A1$  process in kinetics. The relative energy between monohydrate A1W and

AW is 20.1 kcal/mol, which is 1.5 kcal/mol higher than its non-hydrated counterpart ( $E_{A1} - E_A$ ), indicating that monohydration disfavors the stability of the noncanonical isomer of adenine. An analysis shows that it is the lower stabilization

**Table 2.** Relative Energy ( $\Delta E$ ), Binding Energy ( $\Delta E_{\text{BE}}^{\text{W}}$ ), and Stabilization Energy ( $\Delta E_{\text{Stab}}$ ) of AW/A1W/A2W and AMW/A1MW/A2MW Complexes (Energy in kcal/mol)

	$\Delta E$	$\Delta E_{\text{BE}}^{\text{M}}$	$\Delta E_{\text{BE}}^{\text{W}}$	$\Delta E_{\text{Stab}}$		$\Delta E$	$\Delta E_{\text{BE}}^{\text{M}}$	$\Delta E_{\text{BE}}^{\text{W}}$	$\Delta E_{\text{Stab}}$
AW	0.0	—	−8.8	−8.2, −8.7 <sup>b</sup>	ANa <sup>+</sup> W	10.3	−48.2	−9.6	−42.4
A2W	9.0, 9.0 <sup>a</sup>	—	−12.2	−11.1, −11.5 <sup>b</sup>	A2Na <sup>+</sup> W	21.7	−39.0	−12.1	−43.0
A1W	20.1	—	−5.8	−5.5	A1Na <sup>+</sup> W	0.0	−67.3	−11.9	−71.1
ACu <sup>+</sup> W	11.2	−90.0	−11.6	−74.1	AK <sup>+</sup> W	7.2	−30.4	−9.5	−30.6
A1Cu <sup>+</sup> W	0.0	−103.9	−13.7	−103.9	A2K <sup>+</sup> W	16.4	−26.3	−11.8	−33.2
AZn <sup>+</sup> W	12.8	−81.8	−12.1	−65.0	A1K <sup>+</sup> W	0.0	−51.4	−11.1	−56.0
A1Zn <sup>+</sup> W	0.0	−97.9	−14.2	−96.4					

<sup>a</sup>From ref 20 (B3LYP/6-311G(d,p)). <sup>b</sup>From ref 15 (RI-MP2/TZVPP).

energy of A1W (2.7 kcal/mol) than AW that leads to the energy increase of A1W.<sup>15</sup> What will happen in the M-W cooperative systems?

**3.3. PT Process in the M-W Cooperative System.** Figure 2 and Table 2 show the structures and energies of these AMW complexes, respectively. Monohydrates with monohydration at the H15 site of the divalent AM complex cannot be obtained because more charges and, as a result, stronger binding ability of the divalent metal ions,<sup>54</sup> will draw and finally bind the water molecule to generate AMW' instead of AMW. AMW' characterizes with the water molecule binding at the metal ion rather than locating between H15 and N1, where it is designed originally. In monovalent metal ion ( $M = \text{Na}^+, \text{K}^+, \text{Cu}^+, \text{Zn}^+$ ) involved AW systems (AMW), the water molecule can locate between H15 and N1 atoms, as originally expected. Two optimization processes respectively for monovalent  $\text{ANa}^+ + \text{W} \rightarrow \text{ANa}^+\text{W}$  and divalent  $\text{ACa}^{2+} + \text{W} \rightarrow \text{ACa}^{2+}\text{W}'$  are taken as examples to exhibit such difference in Figure S6 in the Supporting Information. Thus, following discussions will focus on the monovalent AMW systems.

For alkali metal ( $\text{Na}^+/\text{K}^+$ )-involved systems, the two-step tautomerization process of  $\text{AMW} \rightarrow \text{A2MW} \rightarrow \text{A1MW}$  still stays in the M-W systems and the first step is also the rate-determining one due to the higher activation energy in the step. However, the activation energy is greatly decreased to less than 20.0 kcal/mol by the monohydration. Interestingly, the monohydration alters the activation energy less than 2.0 kcal/mol in the second one. This indicates that monohydration at the H15 site still retains the first step as a rate-determining one although it greatly decreases the activation energy and enhances the reaction rate of the process. The water molecule in the tautomerization processes of  $\text{AMW} \rightarrow \text{A2MW} \rightarrow \text{A1MW}$  serves as a bridge between H15 and N1 and plays a dual role, the receptor and donor of proton. As a result, the activation energy of PT is decreased. In other words, monohydration would improve the tautomerization of  $\text{AM} \rightarrow \text{A1M}$  in kinetics. By contrast with the rate-determining step in the  $\text{AW} \rightarrow \text{A2W} \rightarrow \text{A1W}$  process, we can find that the alkali metal ion has a subversive effect on it; i.e., the rate-determining step in  $\text{AMW} \rightarrow \text{A2MW} \rightarrow \text{A1MW}$  becomes the second one,  $\text{A2MW} \rightarrow \text{A1MW}$ , due to alkali metal binding.

For the complexes involving univalent transition metal ion, similar phenomenon is also observed. For example, monohydration greatly reduces the activation energy of  $\text{ACu}^+\text{W} \rightarrow \text{A1Cu}^+\text{W}$  process by 31.1 kcal/mol relative to that of non-hydrated  $\text{ACu}^+ \rightarrow \text{A1Cu}^+$  one. The activation energy is still higher slightly than that in the determining-rate step of alkali-metal-involved  $\text{AMW} \rightarrow \text{A2MW}$  processes, which elucidates that monohydration is less effective in improvement of the

reactivity of transition-metal-ion-involved systems than of alkali-metal-ion-involved ones.

From the point of thermodynamics, hydration will extend the gap of relative energy between A1M and AM, and the gaps of the systems involving transition metal ions are larger than those of the ones involving alkali metal ions. For example, the relative energy between  $\text{A1Cu}^+\text{W}$  and  $\text{ACu}^+\text{W}$  is 11.2 kcal/mol, larger than those between  $\text{ACu}^+$  and  $\text{A1Cu}^+$  (9.1), and between  $\text{A1Na}^+\text{W}$  and  $\text{ANa}^+\text{W}$  (10.3), indicating that the cooperative effect of M-W can further strengthen the stability of the A1 isomer and the strength in the transition-metal-ion-involved systems is over the alkali-metal-ion-involved ones.

**Metal Ion Effect on the Binding Energy of Metal Ion to A/A1/A2.** Without metal ion binding, the affinity energy of water at the H15 site of A, A1, and A2 is −8.8, −12.2, and −5.8 kcal/mol, respectively. The corresponding energies in AW and A1W determined by Hanus et al.<sup>15</sup> were −8.7 and −11.5 kcal/mol, respectively, in good consistency with our data. The corresponding H15–O16 distances are 1.949, 1.863, and 1.942 Å, which also relate closely to the fact that the stronger the affinity, the shorter the H15–O16 distance. With metal ion binding, however, the affinity energy of water and the H15–O16 distance alter drastically. For example, the affinity energies of water in  $\text{ANa}^+\text{W}/\text{A2Na}^+\text{W}/\text{A1Na}^+\text{W}$  are −9.6, −12.1, and −11.9 kcal/mol, and the corresponding H15–O16 distances are 1.825, 1.743, and 1.863 Å, respectively. The corresponding distances and energies in  $\text{AK}^+\text{W}/\text{A2K}^+\text{W}/\text{A1K}^+\text{W}$  are 1.838, 1.768, and 1.865 Å, and −9.5, −11.8, and −11.1 kcal/mol, respectively, implying that the metal ion binding strengthens the affinity of the water molecule. For  $\text{A1Cu}^+\text{W}$  and  $\text{A1Zn}^+\text{W}$ , their affinity energies of water are −13.7 and −14.2 kcal/mol, larger by 2.1 kcal/mol than their  $\text{ACu}^+\text{W}$  and  $\text{AZn}^+\text{W}$  counterparts. Hence, the larger affinity of water in the A1MW complexes is another contribution to the stronger stability of the A1 than that of A isomer in the M-W systems.

**Monohydration Effect on the Binding Energy of Metal Ion to A/A1/A2.** Results in Table 2 also show that  $\text{Na}^+$  binding energies in  $\text{ANa}^+\text{W}/\text{A2Na}^+\text{W}/\text{A1Na}^+\text{W}$  are −48.2, −39.0, and −67.3 kcal/mol, respectively, stronger by 3.6, 1.3, and 6.5 kcal/mol than that in  $\text{ANa}^+/\text{A2Na}^+/\text{A1Na}^+$ , indicating that monohydration can enhance the binding strength of metal ion to the adenine and the most obvious enhancement occurs in the A1M isomers. The result accounts for the fact that the A1 isomer would be more stable than the A one in the M-W systems from the binding energy of metal ion point of view. Similar phenomena are also observed in other metal ion bound complexes. On the whole, monohydration enhances the binding strength of metal ion relative to that in the non-hydrated counterparts. It does not alter the ordering of binding strength, however.

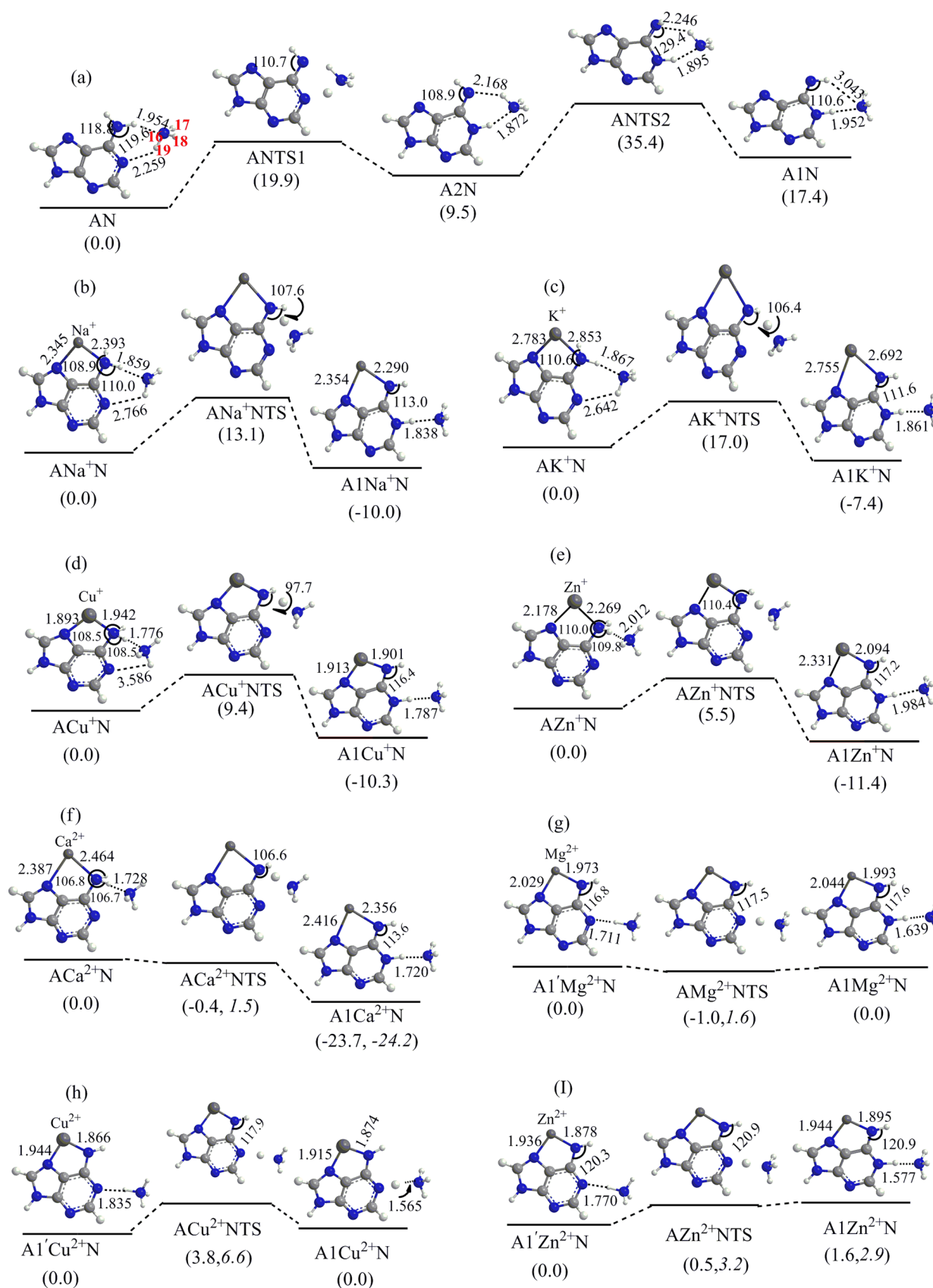


**Figure 3.** Structures and ZPVE-corrected relative energies (in parentheses) in tautomerization processes of AMN → A1MN. Italic data in parentheses denote those relative energies without ZPVE correction. Energy in kcal/mol, distance in angstroms, and angle in degrees.

**3.4. Intramolecular PT Process in the M-N Cooperative Systems.** As a model of the key functional group of

protein, peptide, or amino acid, ammonia can also serve as a receptor and donor of proton, indicating a potential inductive



factor for  $A \rightarrow A1$  tautomerization. Moreover, the interaction between an amino acid and a base is a basic one in the simulation of protein–RNA/DNA interaction<sup>60,61</sup>. However, few reports on such study are observed except that Wu et al.<sup>19</sup> had probed the tautomerization reaction of protonated uracil and thymine induced by an ammonia molecule.

**Intramolecular PT Process in N-Systems.** Figure 3 displays the intramolecular PT processes assisted by an ammonia molecule as well as by M–N. Obviously, the PT process of  $AN \rightarrow A2N \rightarrow A1N$  is very similar to that of  $AW \rightarrow A2W \rightarrow A1W$  in activation energy (35.4 versus 35.9 kcal/mol) and in the rate-determining step (the second step). If the base is protonated, then the ammonia assisted PT is a facile process,<sup>19</sup> and the activation energy would decrease greatly. This further confirms our expectation that N–M system would favor the tautomerization of  $A \rightarrow A1$ . Both  $A1N$  and  $A1W$  are higher in energy than their  $AN$  and  $AW$  (see part a in Figure 3) systems. In absolute value, the energy of  $A1N$  is 17.4 kcal/mol more than that of the  $AN$ , whereas the relative energy for  $A1W$  and  $AW$  is 20.3 kcal/mol and for  $A1$  and  $A$  is 18.6 kcal/mol, indicating that an ammonia rather than a water molecule favors the stability of the  $A1$  isomer.

**Intramolecular PT Process in the M–N Cooperative System.** Once a metal ion is bound, the two-step reaction of  $AN \rightarrow A2N \rightarrow A1N$  becomes a one-step one,  $AMN \rightarrow A1MN$ . This differs from the case in  $AMW \rightarrow A2MW \rightarrow A1MW$  processes. Especially, what we must bring to the attention is that Figure 4 manifests that the tautomerization of  $AMN \rightarrow$

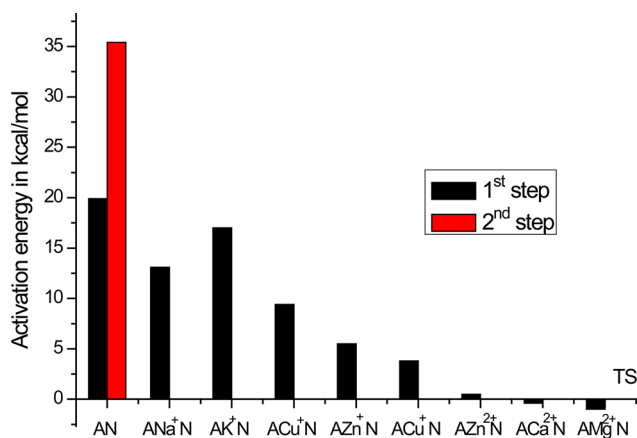


**Figure 4.** Activation energies of tautomerization processes in both  $AN \rightarrow A2N \rightarrow A1N$  and  $AMN \rightarrow A1MN$ . Energy in kcal/mol.

$A1MN$  process becomes easier and easier along with the order of  $M = K^+, Na^+, Cu^+, Zn^+, Cu^{2+}, Zn^{2+}, Ca^{2+}$ , and  $Mg^{2+}$ . Surprisingly, the activation energies in  $AMg^{2+}/Ca^{2+}N \rightarrow A1Mg^{2+}/Ca^{2+}N$  processes become negative values after the ZPVEs are included, indicating that the corresponding processes are spontaneous tautomerization ones.

Two sets of key distances in the TSs of these processes are listed in Table 4. They are N10–H15, H15–N16, and H19–N16 and H19–N1 (refer to labels of N16, H19 in  $AN$ ), respectively. The first set of distances expresses the H15 transfer from the N10 site of adenine to the N16 of the ammonia, and the second one stands for the transfer of H19 from the ammonia to the N1 site of adenine. Results show that H15–N10 and H15–N16 distances are 1.637 and 1.098 Å, respectively, in ANTS. Once a univalent metal ion is bound, they will be shortened to the ranges of 1.508–1.598 and

1.167–1.138 Å ( $AMNTS$ ), respectively. If a divalent  $Ca^{2+}$  is bound, then the two distances are further compressed into 1.326 and 1.313 Å (see  $ACa^{2+}NTS$ ), respectively. These distance data in combination with those in Figure 3 illustrate that H15 is first to transfer to the N16 site and then H19 transfers to the N1 site in the  $AN$ ,  $AM'N$  ( $M'$  refers to the univalent metal ion) and  $ACa^{2+}N$  complexes. That is, it is a sequential PT process and the driving force of PT decreases along with the charge increasing, confirmed by the increased H15–N16/H19–N1 distance or shortened N10–H1/H19–N16 distance. For the divalent  $ACa^{2+}$ , it would be unstable once the ammonia approaches to the H15 site and  $ACa^{2+}N$  will turn into  $A1Ca^{2+}N$  spontaneously due to  $-0.4$  kcal/mol TS energy and  $-23.7$  kcal/mol relative energy of  $A1Ca^{2+}N$ .

Instead of  $[AM]^{2+} \cdot [NH_3]$  form in  $ACa^{2+}N$ , the optimized structures of  $AMg^{2+}N$ ,  $ACu^{2+}N$ , and  $AZn^{2+}N$  become the  $[AM-H]^+ \cdot [NH_4]^+$  form (see parts g, h, i, in Figure 3), in which H15 of adenine transfers to the ammonia, forming a deprotonated  $[AM-H]^+$  species and cationic  $[NH_4]^+$  species, and the cationic  $NH_4^+$  is attracted to the N1 site by using H19 of the  $NH_4^+$  as a H-bond bridge. Therefore, we would like to define them as  $A1'MN$ , as analogues of  $A1MN$ . To view these PT processes clearly, Figures S1–S3 in the Supporting Information display their PESs and corresponding structural changes along with the increase of H15–N10 distance. These figures show clearly that H15 transfer is instantaneous and free, whereas H19 transferring from the N16 ( $NH_4^+$ ) to the N1 site in the  $A1'MN \rightarrow A1MN$  process will consume energy. In detail, it will require 1.6 kcal/mol activation energy for the  $A1'Mg^{2+}N \rightarrow A1Mg^{2+}N$  process. If the ZPVE is included, the activation energy will become  $-1.0$  kcal/mol and is lower than the energy of either  $A1'Mg^{2+}N$  or  $A1Mg^{2+}N$ , indicating that the TS energy in such system is very sensitive to the ZPVE correction and location of H19 at between  $[AMg-H]^+$  and  $NH_3$  rather than at either species is more favorable to the stability of the complex. Thus, a preferred  $A1' \leftrightarrow A1$  resonating structure,  $[AMg-H]^+ \cdots H19^+ \cdots NH_3$  is probable. In fact, the lower-energy TS structure was once observed in the isomerization process of both protonated uracil–ammonia complexes<sup>19</sup> and the protonated amino acid–ammonia complexes.<sup>71</sup> For the  $A1'Cu^{2+}N \rightarrow A1Cu^{2+}N$  process, TS has larger ZPVE-corrected energies (3.8 kcal/mol) than its reactant and product, indicating that H19 must locate at either  $ACu^+-H$  species (correspond to  $A1Cu^{2+}N$ ) or the  $NH_3$  species (correspond to  $A1'Cu^{2+}N$ ). Both  $A1'Cu^{2+}N$  and  $A1Cu^{2+}N$  are stable and equal in energy, and their major distinction in structure lies in H19 location. For the  $A1'Zn^{2+}N \rightarrow A1Zn^{2+}N$  process, TS energy of 3.2 kcal/mol is obtained, which is higher than those of reactant and product. With inclusion of the ZPVE, the relative energy order becomes  $A1'Zn^{2+}N$  (0.0) < TS (0.5) <  $A1Zn^{2+}N$  (1.6 kcal/mol), indicating the  $A1'Zn^{2+}N$  structure is preferred.

In a word, H19 in the four divalent complexes prefers to locate at the N1 site for  $M = Ca^{2+}$ , N16 site for  $M = Zn^{2+}$ , between N1 and N16 for  $M = Mg^{2+}$ , and either N1 or N16 for  $M = Cu^{2+}$ . Comparing with the activation energies in the corresponding processes of either M or M–W systems, we can observe from Figures 3 and 4 that the catalytic effect of ammonia on the PT in these divalent metal involved systems is excellent.

Table 3 lists the relative energy, binding energy, and stabilization energy of these  $AMN$  complexes. Results shows that the stability order is still  $A1MN > AMN$ . It is more interesting that these  $AMN$  complexes are almost comparable



**Table 3.** Relative Energy ( $\Delta E$ ), Binding Energy ( $\Delta E_{\text{BE}}^{\text{W}}$ ), and Stabilization Energy ( $\Delta E_{\text{Stab}}$ ) of AN/A1N/A2N and AMN/A1MN Complexes (Energies in kcal/mol)<sup>a</sup>

	$\Delta E$	$\Delta E_{\text{BE}}^{\text{M}}$	$\Delta E_{\text{BE}}^{\text{N}}$	$\Delta E_{\text{Stab}}$		$\Delta E$	$\Delta E_{\text{BE}}^{\text{M}}$	$\Delta E_{\text{BE}}^{\text{N}}$	$\Delta E_{\text{Stab}}$
AN	0.0		−7.5	−7.1	ACa <sup>2+</sup> N	24.2, 22.2	−148.3	−23.3	−131.8
A2N	9.1		−10.2	−9.7	A1Ca <sup>2+</sup> N	0.0	−173.7	−23.6	−174.8
A1N	17.9		−8.1	−7.5					
ANa <sup>+</sup> N	10.4	−51.9	−11.4	−44.1	A1'Mg <sup>2+</sup> N	0.0	−267.8	21.9	−215.1
A1Na <sup>+</sup> N	0.0	−67.5	−14.4	−73.0	A1Mg <sup>2+</sup> N	0.0, −0.2	−237.5	−28.1	−232.8
AK <sup>+</sup> N	7.6	−32.7	−10.8	−31.7					
A1K <sup>+</sup> N	0.0	−51.5	−13.4	−57.8	A1'Cu <sup>2+</sup> N	0.0	−369.4	36.1	−307.6
ACu <sup>+</sup> N	10.5	−92.0	−15.4	−76.9	A1Cu <sup>2+</sup> N	0.0, 0.1	−339.2	−45.1	−325.5
A1Cu <sup>+</sup> N	0.0	−104.6	−16.9	−106.2					
AZn <sup>+</sup> N	11.7	−82.6	−14.0	−67.2	A1'Zn <sup>2+</sup> N	0.0	−326.4	27.5	−268.6
A1Zn <sup>+</sup> N	0.0	−97.3	−15.5	−97.7	A1Zn <sup>2+</sup> N	2.9, 0.1	−292.8	−31.7	−283.3

<sup>a</sup>Data in italics are from the M062x/6-311++G(d,p) calculations.**Table 4.** H-Bond Distances (in Å) of ANT51 and AMNTS in AN → A1N and AMN → A1MN Processes

	ANTS1	ANa <sup>+</sup> NTS	AK <sup>+</sup> NTS	ACu <sup>+</sup> NTS	AZn <sup>+</sup> NTS	ACa <sup>2+</sup> NTS	AMg <sup>2+</sup> NTS	ACu <sup>2+</sup> NTS	AZn <sup>2+</sup> NTS
N10–H15	1.637	1.598	1.624	1.585	1.508	1.326			
H15–N16	1.098	1.138	1.131	1.133	1.167	1.313			
H19–N16	1.171	1.038	1.043	1.032	1.028	1.025	1.313	1.399	1.381
H19–N1	1.473	2.101	2.030	2.280	2.451	2.693	1.306	1.222	1.245

to those of AMW ones in the relative energy, implying the similar effect of W and N to the stability of these AM isomers. For example, the energy difference between ANa<sup>+</sup>W and A1Na<sup>+</sup>W is 10.0 kcal/mol, whereas that between ANa<sup>+</sup>N and A1Na<sup>+</sup>N is 10.0 kcal/mol, likewise. The parallel differences between AK<sup>+</sup>W and A1K<sup>+</sup>W (7.4) and between AK<sup>+</sup>N and A1K<sup>+</sup>N (7.1) again support this point. Calculated stabilization energies of A1MN (M = Na<sup>+</sup>, K<sup>+</sup>, Cu<sup>+</sup>, Zn<sup>+</sup>, Ca<sup>2+</sup>) are 28.9, 26.1, 29.3, 30.5, and 43.0 kcal/mol, respectively, stronger than their corresponding AMN isomers. The stabilization energy order is in good accord with the relative energy order. A sudden change of relative energy occurs when M = Cu<sup>2+</sup>, Zn<sup>2+</sup>, Mg<sup>2+</sup>, obtained by B3LYP, followed by M062X corroboration. In detail, the A1'MN and A1MN are equal in energy when M = Cu<sup>2+</sup> or Mg<sup>2+</sup>. There is only 1.6 kcal/mol difference between A1'Zn<sup>2+</sup>N and A1Zn<sup>2+</sup>N. Figure 3 accounts for the origin of these changes. Such changes derive from that AMN turns into A1'MN spontaneously when an ammonia is introduced and the structural distinction between A1'MN and A1MN mainly lies in H19 location (i.e., N1 or N16 site). Among these divalent AMN complexes, ACa<sup>2+</sup>N is an exception because its NH<sub>3</sub> species still attaches at the H15 site of N10 and does not transfer to the N1 site when ACa<sup>2+</sup>N is formed. Thus, ACa<sup>2+</sup>N is 24.2 kcal/mol larger than A1Ca<sup>2+</sup>N in energy.

**Metal Ion Effect on the N...A/A1 Binding and N Effect on the M...A/A1 Binding.** Without metal ion bound, the binding energy between ammonia and the A/A1 are −7.5 and −8.1 kcal/mol, whereas the parallel energies between water and A/A1 are −8.8 and −5.8 kcal/mol, respectively. Thus, ammonia binding improves the stability of A1 more than A, whereas monohydration effect is opposite. When a metal ion is introduced, the binding energy of the ammonia increases a little. For example, the binding energy between AM (M = Na<sup>+</sup>, K<sup>+</sup>, Cu<sup>+</sup>, Zn<sup>+</sup>) and ammonia is in the range of −10.5 to −15.0 kcal/mol, while that between A1M and ammonia is in the range of −13.4 (K<sup>+</sup>) to −16.9 (Cu<sup>+</sup>) kcal/mol (Table 3). It indicates that the introduction of the metal cation promotes the binding of ammonia to A/A1 and the promotion in A1 (A1MN) is

more notable. Experimental determination of −17.5 kcal/mol binding energy in N...AH<sup>+</sup> also verifies this conclusion.<sup>19</sup> In divalent A1MN (M = Ca<sup>2+</sup>, Mg<sup>2+</sup>, Zn<sup>2+</sup>, and Cu<sup>2+</sup>), the binding energy of ammonia is −23.6, −28.1, −31.7, and −45.7 kcal/mol, respectively, far larger than those in univalent A1MN (M = Na<sup>+</sup>, K<sup>+</sup>, Zn<sup>+</sup>, and Cu<sup>+</sup>) complexes, which is associated closely with the more charge transfer of these divalent metal ions. For example, Table S1 in the Supporting Information reveals that the charge transfer of Cu<sup>2+</sup> in A1Cu<sup>2+</sup>N is 0.84 to its A1N ligand, twice as much (0.42) as that of Cu<sup>+</sup> in A1Cu<sup>+</sup>N, implying that more charge transfer from divalent metal ion is more favorable to the ammonia binding. Mulliken charge densities (Table S1) of these divalent metal ions decrease along with the ordering of Ca<sup>2+</sup> (1.54), Mg<sup>2+</sup> (1.25), Zn<sup>2+</sup> (1.20), and Cu<sup>2+</sup> (1.16), indicating there is increased charge transfer to the bound ligand (A1N). The corresponding charge density in the A1 and N species does increase gradually along with above metal ion ordering. The ordering strictly conforms to their binding strength, signifying that greater the charge transfer of the metal ion, greater the binding strength of ammonia.

For those divalent AMN reactants, both Table 3 and Table S1 also show that greater charge transfer of metal ion leads to more binding strength of N. However, except ACa<sup>2+</sup>N the other three A1'MN complexes have positive binding energies of N...A1'M interaction, which are unlike their A1MN product. Comparisons show that H15 in ACa<sup>2+</sup>N still binds at the N10 instead of N1 when it is attached by an ammonia molecule, as it does in the system involving monovalent metal ion. Thus, the negative binding energy (−23.3 kcal/mol) between the ACa<sup>2+</sup> and NH<sub>3</sub> species mainly derives from the local electrostatic attraction. Two bound species become [AM-H]<sup>+</sup>·[NH<sub>4</sub>]<sup>+</sup> and form, however, a mutual repulsive structure in AMg<sup>2+</sup>N, ACu<sup>2+</sup>N, and AZn<sup>2+</sup>N, and thus positive energies are created (see  $\Delta E_{\text{BE}}^{\text{N}}$  in Table 3). Data in Table S1 show that the charge densities on [AM-H]<sup>+</sup> and [NH<sub>4</sub>]<sup>+</sup> species are 1.16 and 0.84 for M = Mg<sup>2+</sup>, 1.13 and 0.87 for M = Cu<sup>2+</sup>, and 1.15 and 0.86 for M = Zn<sup>2+</sup>, respectively, which verify the above analysis. In the divalent AMN complexes, charge transfers from the four metal

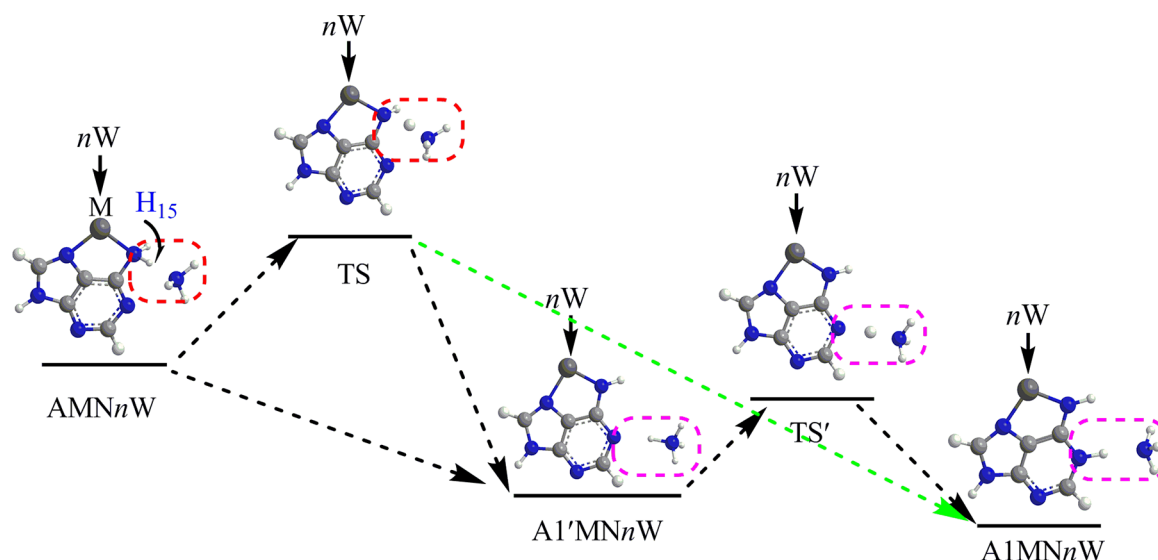


**Figure 5.** Tautomerization processes of  $AMN \rightarrow A1MN$  regulated by microhydration ( $nW$ ,  $n = 1-4$ ), in which  $H_{15}$  shift is displayed in the red dotted line from the  $N_{10}$  site to  $NH_3$  group, then to  $N_1$  site of adenine.

**Table 5.** Relative Energies (kcal/mol) of  $AMN_nW \rightarrow A1MN_nW$  Processes ( $n = 1-4$ )<sup>a</sup>

<i>n</i>								
1	TS	A1CaNW	TS	A1MgNW	TS	A1ZnNW	TS	A1CuNW
	−0.2	−20.8	−1.3	−21.4	−1.6	−0.7	−0.5	−0.8
	1.7	−21.1	0.1	−21.9	−1.4	−0.9	1.8	0.3
2	TS	A1CaN2W	TS	A1MgN2W	TS	A1ZnN2W	TS	A1CuN2W
	1.2	−19.0	−0.3	−20.2	−0.9	−19.5	−1.2	−20.1
	3.2	−19.4	1.6	−20.4	1.1	−19.7	0.8	−20.3
3			TS	A1MgN3W	TS	A1ZnN3W	TS	A1CuN3W
			−	−11.9	0.3	−16.5	0.6	−17.7
			−	−12.1	2.1	−17.1	2.4	−18.2
4			TS	A1MgN4W				
			4.5	−16.2				
			6.3	−16.7				

<sup>a</sup>Data in italics are not included ZPVE corrections. The positive ZPVE-corrected activation energies are highlighted in bold.

ions are 0.46 ( $Ca^{2+}$ ), 0.80( $Mg^{2+}$ ), 0.84( $Zn^{2+}$ ), and 1.02( $Cu^{2+}$ ), respectively. From these data, we can suppose arbitrarily that 0.5 charge transfer would be a threshold for their structures to become  $[AM]^{2+} \cdot [NH_3]$  or  $[AM-H]^+ \cdot [NH_4]^+$  form (like  $A1'M^{2+}N$ ).

In turn, ammonia introduction will also influence the binding of  $M$  to  $A/A1$ . Table 3 reveals that the introduction enhances the univalent  $A \cdots M$  binding in the range of  $-4.2$  ( $AK^+N$ ) to  $-11.6$  kcal/mol ( $ACu^+N$ ). The corresponding enhancement in  $A1 \cdots M$  becomes  $-5.7$  ( $A1K^+N$ ) to  $-8.9$  kcal/mol ( $A1Cu^+N$ ), and in the divalent  $A \cdots M$  and  $A1 \cdots M$  binding are  $-20.6$  ( $ACa^{2+}N$ ) to  $-101.4$  kcal/mol ( $A1'Cu^{2+}N$ ) and  $-16.7$  ( $A1Ca^{2+}N$ ) to  $-38.1$  kcal/mol ( $A1Cu^{2+}N$ ), respectively. These data signify that ammonia introduction increases all these ion binding and the increase is more in the divalent cation involved systems.

**3.5. Intramolecular PT Process in the  $M-N_nW$  ( $n = 1-4$ ) Cooperative Systems.** Due to the excellent catalytic effect of the  $M-N$  cooperation on the tautomerization of divalent  $A \rightarrow A1$  process, we expand our discuss to further probe microhydration on these  $M-N$  systems at the level of M062x/6-311++G(d,p) so that a more practical surrounding condition can be investigated. As a divalent metal ion in vivo, it is generally multi-coordinated by surrounding active sites or

groups, such as water.<sup>72</sup> Thus mono-, di-, tri and tetrahydration at the divalent metal ion are further considered to investigate the changes of activation energy in these PT or tautomerization processes. The microhydration at the metal ion not only affects the activation energy of PT but also the noncovalent interactions between the proton and either ammonia or deprotonated adenine  $A$ . Thus, M062x instead of B3LYP would be better method to perform such investigation.<sup>67-69</sup> The corresponding structures are shown in the Figure S7 of the Supporting Information. These tautomerization processes are condensed in Figure 5.

Compare to the monovalent  $M-N$  systems, the marked difference for divalent  $M-N$  ones is their two charges, thus hydration at the metal ion would reduce the charge density on the adenine from the divalent metal ion binding and regulate the catalytic effect of the  $N-M$  cooperation on the  $A \rightarrow A1$  tautomerization process. Our following aim is to ferret out the hydrated number, which can turn the spontaneous tautomerization process into a compulsory one.

**$M-NW$  Cooperative Systems.** Table 5 lists the relative energies of these  $AMN_nW \rightarrow A1MN_nW$  processes ( $n = 1-4$ ), in which the activation energies are highlighted. For monohydration at the metal ion, the activation energy in the  $ACa^{2+}NW \rightarrow A1Ca^{2+}NW$  process becomes  $-0.2$  kcal/mol,

indicating that monohydration cannot keep the reactant  $\text{ACa}^{2+}\text{NW}$  stable yet, and the reactant will degenerate into  $\text{A1Ca}^{2+}\text{NW}$  spontaneously. Relative to the non-hydrated case ( $-0.4$  kcal/mol), the monohydration increases the potential of the  $\text{ACa}^{2+}\text{N}$  structure. Without ZPVE, the activation energy turns into a positive value ( $1.7$  kcal/mol), however, implying a strong tunneling effect still remains in the monohydrated case. Similar tunneling effect is also observed in the  $\text{AMg}^{2+}\text{NW} \rightarrow \text{A1Mg}^{2+}\text{NW}$  process. Differently, monohydration can keep the  $\text{AMg}^{2+}\text{N}$  stable if the ZPVE is not included; otherwise, the ammonia molecule will capture the H15 from the N10 site and bind to the N1 site (as  $\text{A'Mg}^{2+}\text{N}$  in Figure 4). It is worthy of note that pure  $\text{Mg-N}$  cooperation only generates A1 formatted adenine complex, whether the ZPVE is included or not. This indicates that monohydration at the Mg site is still insufficient to remain the A-formatted adenine stable, although the monohydration greatly increases its stability. In the transition metal ion involved complexes, the energy difference between  $\text{A1Zn}^{2+}\text{NW}$  and  $\text{AZn}^{2+}\text{NW}$ , and the difference between  $\text{A1Cu}^{2+}\text{NW}$  and  $\text{ACu}^{2+}\text{NW}$  are  $0.7$  and  $0.8$  kcal/mol, respectively, indicating that both isomeric complex structures are similar in stability. A comparison for their geometries shows that H15 has transferred closely to the N1 site ( $\text{NH}_3$ ) from initial N10 site, and is in  $\text{NH}_4^+$  format to H-bond to the N1 site of the  $\text{ACu}^{2+}/\text{Zn}^{2+}\text{N}$ . According to the definition of  $\text{A1'MN}$  above, the monohydrates  $\text{ACu}^{2+}\text{NW}$  and  $\text{AZn}^{2+}\text{NW}$  here become into  $\text{A1'Cu}^{2+}\text{NW}$  and  $\text{A1'Zn}^{2+}\text{NW}$ , which hold similar structures both in stability and in geometry to their  $\text{A1Cu}^{2+}\text{NW}$  and  $\text{A1Zn}^{2+}\text{NW}$  counterparts, respectively. The slight difference in geometry mainly derives from that H15 is closer to N1 site or  $\text{NH}_3$  group. Our above calculations for the tautomerization of divalent  $\text{A1'MN} \rightarrow \text{A1MN}$  have confirmed that the process only either needs several kcal/mol activation energy or is free. This indicates that H15 dissociation from N10 site of adenine A instead of H15 transfer from N1 site to the  $\text{NH}_3$  group is the rate-determining step for the  $\text{AMN} \rightarrow \text{A1MN}$  process. Thus, the  $\text{A1'MNnW} \rightarrow \text{A1MNnW}$  step is disregarded deliberately in the following discussion for the  $\text{AMNnW} \rightarrow \text{A1MNnW}$  process, as shown in the green arrow in Figure 5.

**M-N2W Cooperative Systems.** Table 5 manifests that dihydration at the metal ion leads to interesting change for the  $\text{AMN} \rightarrow \text{A1MN}$  tautomerization. Among the four  $\text{AMN2W} \rightarrow \text{A1MN2W}$  processes ( $\text{M} = \text{Ca}^{2+}, \text{Mg}^{2+}, \text{Zn}^{2+}, \text{and Cu}^{2+}$ ),  $\text{ACa}^{2+}\text{N2W} \rightarrow \text{A1Ca}^{2+}\text{N2W}$  process is absolutely outstanding as the TS becomes a positive value ( $1.2$  kcal/mol) after ZPVE correction. This signifies that dihydration at the Ca site would result in stable  $\text{ACa}^{2+}\text{N2W}$ . In other words, dihydration can keep the  $\text{Ca}^{2+}\text{-N}$  cooperative A stable. In contrast, dihydration cannot make the  $\text{Mg}^{2+}\text{-N}$  cooperative A stable, although it further increases the relative stability of  $\text{AMg}^{2+}\text{N2W}$  to that of  $\text{A1Mg}^{2+}\text{N2W}$ . The relative value is  $1.2$  kcal/mol more than that in the monohydrated process without ZPVE corrections. For two transition metal ion involved systems, marked improvement comes from the fact that their  $\text{AZn}^{2+}/\text{Cu}^{2+}\text{N2W}$  structures can be stable without ZPVE corrections. In contrast, the monohydrated  $\text{AZn}^{2+}/\text{Cu}^{2+}\text{N}$  one cannot and will directly transform into their  $\text{A1Zn}^{2+}/\text{Cu}^{2+}\text{N}$  product without barrier.

**M-N3W and  $\text{Mg}^{2+}\text{-N4W}$  Cooperative Systems.** On further hydration at the metal-ion site for the latter three  $\text{AMN3W} \rightarrow \text{A1MN3W}$  processes ( $\text{M} = \text{Mg}^{2+}, \text{Zn}^{2+}, \text{and Cu}^{2+}$ ), new phenomena arise. Activation energies in two transition metal ion involved  $\text{AMN3W} \rightarrow \text{A1MN3W}$  processes first become

positive values ( $0.3/\text{Zn}^{2+}; 0.6/\text{Cu}^{2+}$  kcal/mol) after their ZPVEs are included, which imply that three water molecules are the least number required to stabilize the such M-N cooperative A structures. Different from the phenomena in two  $\text{AZn}^{2+}/\text{Cu}^{2+}\text{N3W}$  complexes, the binding of the third water to  $\text{Mg}^{2+}$  attracts the  $\text{NH}_3$  group apart from its initial binding site (N10) to one of the water molecule (see  $\text{AMg}^{2+}\text{N3W}$  in Figure S7 in the Supporting Information). As a result, the expected catalysis of  $\text{NH}_3$  group for the H16 transfer (from N10 site to N1 site) will lose. This phenomenon also indicates that more hydration at the Mg site is required to shield such strong absorption to the  $\text{NH}_3$  group. Thus, the tetrahydrated case is considered. Results show that tetrahydration at the Mg site can not only hold the  $\text{NH}_3$  group at the H16 site but also keep the  $\text{AMg}^{2+}\text{N4W}$  structure stable. The activation energy in the  $\text{AMg}^{2+}\text{N4W} \rightarrow \text{A1Mg}^{2+}\text{N4W}$  process first turns into positive value ( $4.5$  kcal/mol), indicating that the least number to keep  $\text{AMg}^{2+}\text{N}$  stable is four in the  $\text{AMg}^{2+}\text{N4W} \rightarrow \text{A1Mg}^{2+}\text{N4W}$  process.

#### 4. CONCLUSIONS

As the most stable isomer of adenine A and its higher-energy isomer A1, being the reactant of the most stable metalated complex A1M, a mass of factors affect the  $\text{A} \rightarrow \text{A1}$  tautomerization. The following important conclusions are drawn.

For the tautomerization process of  $\text{A} \rightarrow \text{A1}$ , metalation can greatly strengthen the stability of the rare A1 isomer and lead it to be more stable than the A isomer, indicating the probable existence in thermodynamics of the A1 isomer under the circumstance of metal coordination. In the view of the kinetics, the tautomerization of  $\text{A} \rightarrow \text{A1}$  becomes more difficult, however, in the metalated case than in the nonmetalated case. On the contrary, W/N attachment favors the  $\text{A} \rightarrow \text{A1}$  tautomerization in kinetics, but disfavors the stability of the rare A1 isomer ( $\text{A1W}$  or  $\text{A1N}$ ) in thermodynamics.

In M-W cooperative cases, the tautomerization process of  $\text{A} \rightarrow \text{A1}$  improves greatly both in thermodynamics and in kinetics. The drawback of such M-W cooperative systems is that the involved M is only limited to the monovalent metal ion and is not suitable for the divalent one. In a divalent M-W cooperative system, stronger binding ability of the metal ion will draw and bind the water molecule directly even if the designed location originally for the water molecule is between the H15 and N1 atoms of the adenine A, in which it can play a bridge role for PT. This indicates divalent M-W cooperation is more favorable than the monovalent one to the  $\text{A} \rightarrow \text{A1}$  tautomerization in thermodynamics but in kinetics.

Substituting N for W of the M-W cooperation, then not only the drawback emerged from M-W cooperative system can be avoided, but also the process of  $\text{A} \rightarrow \text{A1}$  tautomerization will become more smooth both in thermodynamics and in kinetics. Moreover, the divalent M-N cooperation can lead to energy-free  $\text{A} \rightarrow \text{A1}$  tautomerization, showing excellent catalytic ability for the tautomerization and probable effortless adenine mutation in the individual DNA base-amino acid interactions.<sup>60</sup>

To inhibit the energy-free  $\text{A} \rightarrow \text{A1}$  tautomerization or adenine mutation in these divalent M-N cooperative systems ( $\text{AMN} \rightarrow \text{A1MN}$ ), the present work also offers valid options for the system involving different metal ions. In detail, binding two water molecules to the  $\text{Ca}^{2+}$  site can keep the A ( $\text{ACa}^{2+}\text{N}$ ) structure stable rather than mutating to A1 ( $\text{A1Ca}^{2+}\text{N}$ ) readily,



whereas the number of water molecules to obtain stable  $\text{ACu}^{2+}\text{N}$ ,  $\text{AZn}^{2+}\text{N}$ , and  $\text{AMg}^{2+}\text{N}$  becomes 3, 3, and 4, respectively. The different numbers of water molecules required indicate that different hydrated schemes should be employed to keep the stability of the different divalent ion involved AMN structures.

In summary, the present work not only opens up an energy-free way to achieve the tautomerization from the most stable isomer to a rare one, but also shows how to regulate and even prevent such unfavorable  $\text{A} \rightarrow \text{A1}$  tautomerization. We hope this information would be valuable in understanding and control of both the point mutation induced by the  $\text{A} \rightarrow \text{A1}$  tautomerization, and as a result of the structure, property, and function of base mispairing.

## ■ ASSOCIATED CONTENT

### ● Supporting Information

Charge density of different parts in the AMN/A1MN and the corresponding TS complexes (Table S1), complete citation for ref 70 (S0), PESs along with changes of the N10-NH<sub>3</sub> distance in  $\text{ACu}^{2+}\text{N}$  (Figure S1-1),  $\text{AMg}^{2+}\text{N}$  (Figure S2-1) and  $\text{AZn}^{2+}\text{N}$  (Figure S3-1), optimized  $\text{ACu}^{2+}\text{N}$  (Figure S1-2),  $\text{AMg}^{2+}\text{N}$  (Figure S2-2) and  $\text{AZn}^{2+}\text{N}$  (Figure S3-2) geometries along with the distance changes of N10-NH<sub>3</sub>, M06-2X/6-311++G(d,p) level optimized course of  $\text{AMg}^{2+}\text{N}$  structure (Figure S2-3), relative energy and structural parameters of complexes in  $\text{A} \rightarrow \text{A2} \rightarrow \text{A1}$  and  $\text{AM} \rightarrow \text{A1M}$  processes (a, b, ..., i) (Figure S4), PESs and several selected corresponding structures during optimization for the reactions of (a)  $\text{A} + \text{Cu}^+ \rightarrow \text{ACu}^+$ , (b)  $\text{A} + \text{Na}^+ \rightarrow \text{ANa}^+$ , (c)  $\text{A2} + \text{Cu}^+ \rightarrow \text{A1Cu}^+$ , and (d)  $\text{A2} + \text{Na}^+ \rightarrow \text{A2Na}^+$  (Figure S5), and for the reactions of (a)  $\text{ANa}^+ + \text{W} \rightarrow \text{ANa}^+\text{W}$  and (b)  $\text{ACa}^{2+} + \text{W} \rightarrow \text{ACa}^{2+}\text{W}'$  (Figure S6), optimized AMNnW, A1MNnW ( $n = 1-4$ ) structures and their transition states (Figure S7) This material is available free of charge via the Internet at <http://pubs.acs.org>.

## ■ AUTHOR INFORMATION

### Corresponding Author

\*E-mail: [chm\\_aihq@ujn.edu.cn](mailto:chm_aihq@ujn.edu.cn).

### Notes

The authors declare no competing financial interest.

## ■ ACKNOWLEDGMENTS

We thank the National Natural Science Foundation of China (NSFC) (No. 20973084) and NSFC-NRF (Korea) Joint Exchange Project (No. 21211140340) as well as Shandong Provincial NSF (No. Y2008B56) for financial support.

## ■ REFERENCES

- (1) Dreyfus, M.; Dodin, G.; Bensaude, O.; Dubois, J. E. *J. Am. Chem. Soc.* **1975**, *97*, 2369–2377.
- (2) Fogarasi, G. *J. Phys. Chem. A* **2002**, *106*, 1381–1390.
- (3) Ha, T.-K.; Keller, M. J.; Gunde, R.; Gunthard, H. H. *J. Mol. Struct. THEOCHEM.* **1996**, *364*, 161–181.
- (4) Ha, T.-K.; Gunthard, H. H. *J. Am. Chem. Soc.* **1993**, *115*, 11939–11950.
- (5) Ha, T.-K.; Keller, H. J.; Gunde, R.; Gunthard, H. H. *J. Phys. Chem. A* **1999**, *103*, 6612–6623.
- (6) Katritzky, A. R.; Karelson, M. *J. Am. Chem. Soc.* **1991**, *113*, 1561–1566.
- (7) Kobayashi, R. *J. Phys. Chem. A* **1998**, *102*, 10813–10817.
- (8) Nir, E.; Janzen, C.; Imhof, P.; Kleinermanns, K.; De Vries, M. S. *J. Chem. Phys.* **2001**, *115*, 4604–4611.
- (9) Nir, E.; Kleinermanns, K.; Grace, L.; de Vries, M. S. *J. Phys. Chem. A* **2001**, *105*, 5106–5110.
- (10) Piacenza, M.; Grimme, S. *J. Comput. Chem.* **2004**, *25*, 83–98.
- (11) Plützer, C.; Kleinermanns, K. *Phys. Chem. Chem. Phys.* **2002**, *4*, 4877–4882.
- (12) Yang, Z.; Rodgers, M. T. *Phys. Chem. Chem. Phys.* **2004**, *6*, 2749–2757.
- (13) Szczesniak, M.; Szczepaniak, K.; Kwiatkowski, J. S.; KuBulat, K.; Person, W. B. *J. Am. Chem. Soc.* **1988**, *110*, 8319–8330.
- (14) Salter, L. M.; Chaban, G. M. *J. Phys. Chem. A* **2002**, *106*, 4251–4256.
- (15) Hanus, M.; Kabeláč, M.; Rejnek, J.; Ryjáček, F.; Hobza, P. *J. Phys. Chem. B* **2004**, *108*, 2087–2097.
- (16) Trygubenko, S. A.; Bogdan, T. V.; Rueda, M.; Orozco, M.; Luque, F. J.; Šponer, J.; Slaviček, P.; Hobza, P. *Phys. Chem. Chem. Phys.* **2002**, *4*, 4192–4203.
- (17) Rejnek, J.; Hanus, M.; Kabeláč, M.; Ryjáček, F.; Hobza, P. *Phys. Chem. Chem. Phys.* **2005**, *7*, 2006–2017.
- (18) Hanus, M.; Ryjáček, F.; Kabeláč, M.; Kubař, T.; Bogdan, T. V.; Trygubenko, S. A.; Hobza, P. *J. Am. Chem. Soc.* **2003**, *125*, 7678–7688.
- (19) Wu, R.; McMahon, T. B. *J. Am. Chem. Soc.* **2007**, *129*, 569–580.
- (20) Gu, J.; Leszczynski, J. *J. Phys. Chem. A* **1999**, *103*, 2744–2750.
- (21) Kim, H. S.; Ahn, D. S.; Chung, S. Y.; Kim, S. K.; Lee, S. J. *Phys. Chem. A* **2007**, *111*, 8007–8012.
- (22) Hu, X.; Li, H.; Liang, W.; Han, S. *J. Phys. Chem. B* **2005**, *109*, 5935–5944.
- (23) Hu, X.; Li, H.; Liang, W.; Han, S. *J. Phys. Chem. B* **2004**, *108*, 12999–13007.
- (24) Mennucci, B.; Toniolo, A.; Tomasi, J. *J. Phys. Chem. A* **2001**, *105*, 4749–4757.
- (25) Gorb, L.; Leszczynski, J. *J. Am. Chem. Soc.* **1998**, *120*, 5024–5032.
- (26) Sukhanov, O. S.; Shishkin, O. V.; Gorb, L.; Podolyan, Y.; Leszczynski, J. *J. Phys. Chem. B* **2003**, *107*, 2846–2852.
- (27) Roitzsch, M.; Lippert, B. *Inorg. Chem.* **2004**, *43*, 5483–5485.
- (28) Šponer, J.; Sabat, M.; Gorb, L.; Leszczynski, J.; Lippert, B.; Hobza, P. *J. Phys. Chem. B* **2000**, *104*, 7535–7544.
- (29) Muñoz, J.; Šponer, J.; Hobza, P.; Orozco, M.; Luque, F. J. *J. Phys. Chem. B* **2001**, *105*, 6051–6060.
- (30) Lippert, B. *Coord. Chem. Rev.* **2000**, *200*–202, 487–516.
- (31) Fonseca Guerra, C.; Bickelhaupt, F. M.; Saha, S.; Wang, F. *J. Phys. Chem. A* **2006**, *110*, 4012–4020.
- (32) Kabeláč, M.; Hobza, P. *J. Phys. Chem. B* **2006**, *110*, 14515–14523.
- (33) Topal, M. D.; Fresco, J. R. *Nature* **1976**, *263*, 285–289.
- (34) Les, A.; Adamowicz, L. *J. Phys. Chem. A* **1989**, *93*, 7078–7081.
- (35) Kryachko, E. S.; Sabin, J. R. *Int. J. Quantum Chem.* **2003**, *91*, 695–710.
- (36) Holbrook, S. R.; Cheong, C.; Tinoco, I., Jr.; Kim, S. H. *Nature* **1991**, *353*, 579–581.
- (37) Shi, K.; Wahl, M.; Sundaralingam, M. *Nucleic Acids Res.* **1999**, *27*, 2196–2201.
- (38) Kryachko, E. S.; Nguyen, M. T. *J. Phys. Chem. A* **2002**, *106*, 9319–9324.
- (39) Kryachko, E. S. *Int. J. Quantum Chem.* **2002**, *90*, 910–923.
- (40) Harris, V. H.; Smith, C. L.; Jonathan Cummins, W.; Hamilton, A. L.; Adams, H.; Dickman, M.; Hornby, D. P.; Williams, D. M. *J. Mol. Biol.* **2003**, *326*, 1389–1401.
- (41) Florián, J.; Leszczyński, J. *J. Am. Chem. Soc.* **1996**, *118*, 3010–3017.
- (42) Russo, N.; Toscano, M.; Grand, A. *J. Am. Chem. Soc.* **2001**, *123*, 10272–10279.
- (43) Rodgers, M. T.; Armentrout, P. B. *J. Am. Chem. Soc.* **2002**, *124*, 2678–2691.
- (44) Florian, J.; Hroudá, V.; Hobza, P. *J. Am. Chem. Soc.* **1994**, *116*, 1457–1460.
- (45) Burnouf, D.; Duane, M.; Fuchs, R. P. *Proc. Natl. Acad. Sci. U.S.A.* **1987**, *84*, 3758–3762.



- (46) Zamora, F.; Kunsman, M.; Sabat, M.; Lippert, B. *Inorg. Chem.* **1997**, *36*, 1583–1587.
- (47) Chifotides, H. T.; Dunbar, K. R. *J. Am. Chem. Soc.* **2007**, *129*, 12480–12490.
- (48) Šponer, J.; Šponer, J. E.; Gorb, L.; Leszczynski, J.; Lippert, B. *J. Phys. Chem. A* **1999**, *103*, 11406–11413.
- (49) Rodgers, M. T.; Armentrout, P. B. *J. Am. Chem. Soc.* **2000**, *122*, 8548–8558.
- (50) Russo, N.; Toscano, M.; Grand, A. *J. Phys. Chem. A* **2003**, *107*, 11533–11538.
- (51) Xing, D.; Tan, X.; Chen, X.; Bu, Y. *J. Phys. Chem. A* **2008**, *112*, 7418–7425.
- (52) Viljanen, J.; Klika, K. D.; Sillanpää, R.; Arpalähti, J. *Inorg. Chem.* **1999**, *38*, 4924–4925.
- (53) Chen, D.; Gregan, F.; Holy, A.; Sigel, H. *Inorg. Chem.* **1993**, *32*, 5377–5384.
- (54) Deubel, D. V. *J. Am. Chem. Soc.* **2008**, *130*, 665–675.
- (55) Chifotides, H. T.; Dunbar, K. R. *Acc. Chem. Res.* **2005**, *38*, 146–156.
- (56) Glassman, T. A.; Cooper, C.; Harrison, L. W.; Swift, T. J. *Biochemistry* **1971**, *10*, 843–851.
- (57) Hu, X.; Li, H.; Zhang, L.; Han, S. *J. Phys. Chem. B* **2007**, *111*, 9347–9354.
- (58) Michalkova, A.; Kosenkov, D.; Gorb, L.; Leszczynski, J. *J. Phys. Chem. B* **2008**, *112*, 8624–8633.
- (59) Li, D.; Ai, H. *J. Phys. Chem. B* **2009**, *113*, 11732–11742.
- (60) Desjarlais, J. R.; Ber, J. M. *Proc. Natl. Acad. Sci. U.S.A.* **1994**, *91*, 11099–11103.
- (61) Lustig, B.; Jernigan, R. L. *Nucleic Acids Res.* **1995**, *23*, 4707–4711.
- (62) Lippert, B. *Prog. Inorg. Chem.* **2005**, *54*, 385–447.
- (63) Becke, A. D. *Phys. Rev. A* **1988**, *38*, 3098–3100.
- (64) Lee, C.; Yang, W.; Parr, R. G. *Phys. Rev. B* **1988**, *37*, 785–789.
- (65) Gonzalez, C.; Schlegel, H. B. *J. Chem. Phys.* **1989**, *90*, 2154–2161.
- (66) Boys, S. F.; Bernardi, F. *Mol. Phys.* **1970**, *19*, 553–566.
- (67) Zhao, Y.; Truhlar, D. G. *Acc. Chem. Res.* **2008**, *41*, 157–167.
- (68) Srinivasadesikan, V.; Sahu, P. K.; Lee, S.-L. *J. Phys. Chem. B* **2012**, *116*, 11173–11179.
- (69) Fang, H.; Kim, Y. *J. Chem. Theory Comput.* **2011**, *7*, 642–657.
- (70) Frisch, M. J.; Trucks, G. W.; Schlegel, H. B.; Scuseria, G. E.; Robb, M. A.; Cheeseman, J. R.; Scalmani, G.; Barone, V.; Mennucci, B.; Petersson, G. A.; et al., *Gaussian 09, Revision A.02*; Gaussian Inc, Wallingford, CT, 2009 (for the complete citation, see Supporting Information)
- (71) Wu, R.; McMahon, T. B. *J. Am. Chem. Soc.* **2008**, *130*, 3065–3078.
- (72) Wakisaka, A.; Watanabe, Y. *J. Phys. Chem. B* **2002**, *106*, 899–901.